

Influence of rotary flexibility of joints on the statics and dynamics of the arch structures

Magdalena ŁASECKA-PLURA^{✉*}, Zdzisław PAWLAK[✉], and Martyna ŻAK-SAWIAK[✉]

Poznan University of Technology, Institute of Structural Analysis, ul. Piotrowo 5, 60-965 Poznań, Poland

Abstract. The paper presents arch structures modeled by finite elements in which the nodes can be flexibly connected. Two-node curved elements with three degrees of freedom at each node were used. Exact shape functions were adopted to obtain stiffness and consistent mass matrices but they were modified by introducing rotational flexibility in the boundary nodes. Calculations of statics and dynamics of arches with different positions of flexible joints and different values of rotational stiffness of the joints were carried out.

Key words: rotational elasticity of joints; arched structures; curved beam element; modal analysis.

1. INTRODUCTION

With technical progress, the requirements for the span of the structure increase for functional and utility reasons. Hence the increasing use of arched structures, which are used in public buildings, industrial constructions, bridge engineering, and underground constructions.

Analytical solutions of arches require a solution of a sixth-order differential equation. Different calculation models of arch structures were adopted. The simplest model is the one in which the effects of shear deformation and compressibility of the axis are ignored, and in the case of dynamics, the influence of rotational inertia is also neglected. In many cases, such a model, also known as the Euler-Bernoulli arch, is sufficient. However, for thick and shallow arches, it is necessary to extend the solution with the influence of shear deformation, axial extensibility, and rotary inertia. It is the so-called Timoshenko arch. Solutions for all combinations of the above cases can be found in [1, 2].

In the case of using the finite element method for analysis, the simplest model is the approximation of the arch curvature with straight elements [3]. However, this approach does not take into account the coupling of differential equations in curved beams and requires a division into a significant number of elements. This is eliminated by using curved elements that can accurately model the geometry. Different functions of interpolating displacements are assumed. Fifth-order polynomials were used in [4], cubic ones in [5], and three different polynomial interpolating functions were used in [6]. Trigonometric functions as interpolating functions were used in [3] and [7]. The exact shape functions (see [7]) obtained in this way make it possible to obtain exact solutions in the nodes in the case of a static

problem. The obtained finite elements are free from the effects of shear and membrane locking.

Different types of arches (parabolic, sinusoidal and elliptical) are presented in [4]. The dynamic analysis of arches with variable cross-sections was considered in [8, 9]. Arches of an arbitrary curve are very often analyzed by using the isogeometric approach. This approach is presented in [10, 11].

In the literature, arch structures with different boundary conditions are considered, also with flexible supports. The closed-form solution to the dynamic problem of the circular arch is presented in [12]. Flexible supports were also taken into account in [13], where the authors presented that flexible supports reduce the frequency of natural vibrations. In [14], the authors proved that the use of flexible supports significantly reduces the damage to underground arch structures.

In this paper, the exact stiffness matrix and consistent mass matrix for a curved element with rotational flexibility of nodes are derived. A similar solution was shown in [15, 16], but for straight elements. The starting point is the well-known solution for a curved element with fixed supports, while the flexible supports are modeled as elastic springs. Nodal displacements and rotations are selected as the primary unknowns, while displacements and rotations at the element ends are eliminated. According to the authors' knowledge, such a solution has not yet been presented for a curved element. Real structures are usually modeled as supported on rigid or pinned supports. In fact, most connections, including internal ones, have some limited flexibility. The solution presented by the authors allows for the analysis of arch structures with flexible external and internal joints.

The derived formulas made it possible to write a computational program, which was used to solve the problem of statics and the eigenproblem of dynamics of arch structures with flexible connections. Then, parametric studies were performed to show the influence of flexibility joints on solutions.

*e-mail: magdalena.lasecka-plura@put.poznan.pl

Manuscript submitted 2022-06-30, revised 2022-11-28, initially accepted for publication 2022-12-28, published in February 2023.

2. FORMULATION OF THE CURVED BEAM ELEMENT WITH ROTATIONAL FLEXIBILITY OF NODES

2.1. Stiffness and mass matrices for curved beam element

A plane two-node curved finite element with six degrees of freedom is considered (Fig. 1) with the radius of curvature R , the angle α , and the length of the element l_e ($l_e = R\alpha$). Exact shape functions [7] are used, based on which an exact stiffness matrix [7] and a consistent mass matrix [17] are obtained for the element with non-flexible nodes. The matrix coefficients take into account the influence of shear flexibility and compressibility of the arch. The stiffness and mass matrices and all the coefficients needed to compute them are given in Appendix A1.

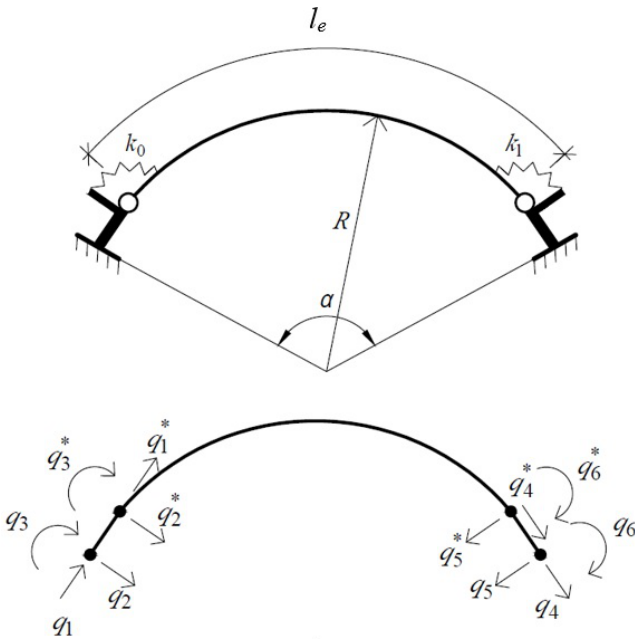


Fig. 1. Curved finite element with flexible connections

The considered element is described by the following properties: E – Young modulus, G – Kirchhoff modulus, I – the moment of inertia and A – area of cross-section. The effect of shear and axial deformation is described by two dimensionless parameters:

$$d = \frac{EI}{\kappa GA} \cdot \frac{1}{l_e^2} = \frac{2(1+\nu)}{\kappa} \left(\frac{i}{l_e}\right)^2, \quad e = \frac{EI}{EA} \cdot \frac{1}{l_e^2} = \left(\frac{i}{l_e}\right)^2, \quad (1)$$

where ν is the Poisson's ratio, κ is the shear factor, and i is the radius of gyration.

2.2. Introduction of flexible joints

The rotational flexibility of element nodes is represented by the stiffnesses k_0 and k_1 (Fig. 1). The considered element is connected to the nodes by flexible rotational elements of infinite stiffness and infinitesimal length. Displacements for an element are marked with an asterisk, while displacements in supports can be written as:

$$q_3 = q_3^* + q_{3s}, \quad q_6 = q_6^* + q_{6s} \quad (2)$$

for rotations, and

$$q_1 = q_1^*, \quad q_2 = q_2^*, \quad q_4 = q_4^*, \quad q_5 = q_5^* \quad (3)$$

for tangential and radial displacements. q_{3s} and q_{6s} denote rotations in flexible supports and can be expressed as follows:

$$q_{3s} = Q_3^* l_e^2 / k_0, \quad q_{6s} = Q_6^* l_e^2 / k_1, \quad (4)$$

where Q_3^* and Q_6^* are the bending moments at the nodes of the curved element.

The relationship between forces and displacements for a curved element is written as:

$$\mathbf{Q}^* = \bar{\mathbf{K}} \mathbf{q}^*, \quad (5)$$

where

$$\mathbf{Q}^* = [Q_1^* \quad Q_2^* \quad Q_3^* \quad Q_4^* \quad Q_5^* \quad Q_6^*]^T, \\ Q_3^* = m_1 = M_1 / l_e, \quad Q_6^* = m_2 = M_2 / l_e$$

is a vector of forces at the ends of the element,

$$\mathbf{q}^* = [q_1^* \quad q_2^* \quad q_3^* \quad q_4^* \quad q_5^* \quad q_6^*]^T, \\ q_3^* = \phi_1 = \varphi_1 l_e, \quad q_6^* = \phi_2 = \varphi_2 l_e$$

is a vector of displacements at the ends of the element and $\bar{\mathbf{K}}$ is the stiffness matrix given in Appendix A1.

Based on equation (5), the following relationship can be written:

$$\begin{bmatrix} Q_3^* \\ Q_6^* \end{bmatrix} = \frac{EI}{l_e^3} \begin{bmatrix} \bar{k}_{31} & \bar{k}_{32} & \bar{k}_{33} & \bar{k}_{34} & \bar{k}_{35} & \bar{k}_{36} \\ \bar{k}_{61} & \bar{k}_{62} & \bar{k}_{63} & \bar{k}_{64} & \bar{k}_{65} & \bar{k}_{66} \end{bmatrix} \mathbf{q}^*, \quad (6)$$

where \bar{k}_{ij} are the elements of the stiffness matrix $\bar{\mathbf{K}}$.

After substituting equations (2) and (3) into (6) the following formula is obtained:

$$\begin{bmatrix} Q_3^* \\ Q_6^* \end{bmatrix} = \frac{EI}{l_e^3} \mathbf{K}_Z \begin{bmatrix} q_1 \\ q_2 \\ q_3 - q_{3s} \\ q_4 \\ q_5 \\ q_6 - q_{6s} \end{bmatrix} \\ = \frac{EI}{l_e^3} \mathbf{K}_Z \begin{bmatrix} q_1 \\ q_2 \\ q_3 \\ q_4 \\ q_5 \\ q_6 \end{bmatrix} - \frac{EI}{l_e^3} \mathbf{K}_Z \begin{bmatrix} 0 \\ 0 \\ q_{3s} \\ 0 \\ 0 \\ q_{6s} \end{bmatrix}, \quad (7)$$

where

$$\mathbf{K}_Z = \begin{bmatrix} \bar{k}_{31} & \bar{k}_{32} & \bar{k}_{33} & \bar{k}_{34} & \bar{k}_{35} & \bar{k}_{36} \\ \bar{k}_{61} & \bar{k}_{62} & \bar{k}_{63} & \bar{k}_{64} & \bar{k}_{65} & \bar{k}_{66} \end{bmatrix}.$$

After using equation (4) and performing some transformations, the following expression is obtained:

$$\begin{bmatrix} Q_3^* \\ Q_6^* \end{bmatrix} = \mathbf{A} \mathbf{q}, \quad (8)$$

where

$$\mathbf{A} = \frac{EI}{l_e^3} \mathbf{B}^{-1} \mathbf{K}_Z, \quad \mathbf{B} = \begin{bmatrix} 1 + \frac{EI}{l_e} \bar{k}_{33} \frac{1}{k_0} & \frac{EI}{l_e} \bar{k}_{36} \frac{1}{k_l} \\ \frac{EI}{l_e} \bar{k}_{63} \frac{1}{k_0} & 1 + \frac{EI}{l_e} \bar{k}_{66} \frac{1}{k_l} \end{bmatrix}.$$

Then, it is possible to write matrix \mathbf{A} in the following form:

$$\mathbf{A} = [a_{ij}]_{2 \times 6}. \quad (9)$$

Vector \mathbf{q}_s can be expressed as:

$$\mathbf{q}_s = \begin{bmatrix} 0 \\ 0 \\ q_{3s} \\ 0 \\ 0 \\ q_{6s} \end{bmatrix} = \begin{bmatrix} 0 \\ 0 \\ Q_3^* l_e^2 / k_0 \\ 0 \\ 0 \\ Q_6^* l_e^2 / k_l \end{bmatrix}, \quad (10)$$

and after substituting Q_3^* and Q_6^* calculated from equation (8) into equation (10), it is possible to describe rotations in flexible supports in the matrix form:

$$\mathbf{q}_s = \mathbf{D} \mathbf{q}, \quad (11)$$

where

$$\mathbf{D} = \begin{bmatrix} 0 & 0 & 0 & 0 & 0 & 0 \\ 0 & 0 & 0 & 0 & 0 & 0 \\ d_{11} & d_{12} & d_{13} & d_{14} & d_{15} & d_{16} \\ 0 & 0 & 0 & 0 & 0 & 0 \\ 0 & 0 & 0 & 0 & 0 & 0 \\ d_{21} & d_{22} & d_{23} & d_{24} & d_{25} & d_{26} \end{bmatrix},$$

$$d_{1i} = \frac{a_{1i} l_e^2}{k_0} = \frac{1}{\Omega} [\bar{k}_{3i} (K_l + \bar{k}_{66}) - \bar{k}_{36} \bar{k}_{6i}],$$

$$d_{2i} = \frac{a_{2i} l_e^2}{k_l} = \frac{1}{\Omega} [\bar{k}_{6i} (K_0 + \bar{k}_{33}) - \bar{k}_{63} \bar{k}_{3i}], \quad \text{for } i = 1, \dots, 6,$$

$$\Omega = K_0 K_l + \bar{k}_{33} K_l + \bar{k}_{66} K_0 + \bar{k}_{33} \bar{k}_{66} - \bar{k}_{36} \bar{k}_{63},$$

$$K_0 = \frac{l_e k_0}{EI}, \quad K_l = \frac{l_e k_l}{EI}.$$

The displacement field for a curved beam with flexible nodes can be approximated by the following functions:

$$w(x) = \mathbf{N}(x) \mathbf{q}^* = \mathbf{N}(x) (\mathbf{I} - \mathbf{D}) \mathbf{q}, \quad (12)$$

where $\mathbf{N}(x)$ is the set of the exact shape function for a curved beam element fixed at both ends [7] and \mathbf{I} is an identity matrix.

Then using the theory of minimum potential energy, the following stiffness matrix for the curved element with flexible nodes can be obtained:

$$\mathbf{K} = (\mathbf{I} - \mathbf{D})^T \bar{\mathbf{K}} (\mathbf{I} - \mathbf{D}) + \mathbf{D}^T \mathbf{S} \mathbf{D}, \quad (13)$$

where

$$\mathbf{S} = \begin{bmatrix} 0 & 0 & 0 & 0 & 0 & 0 \\ 0 & 0 & 0 & 0 & 0 & 0 \\ 0 & 0 & k_0 & 0 & 0 & 0 \\ 0 & 0 & 0 & 0 & 0 & 0 \\ 0 & 0 & 0 & 0 & 0 & 0 \\ 0 & 0 & 0 & 0 & 0 & k_l \end{bmatrix}.$$

Based on the previous derivation, a consistent mass matrix can be calculated using the following formula:

$$\mathbf{M} = (\mathbf{I} - \mathbf{D})^T \bar{\mathbf{M}} (\mathbf{I} - \mathbf{D}), \quad (14)$$

where $\bar{\mathbf{M}}$ is mass matrix given in Appendix A1.

The static problem is formulated as follows:

$$\mathbf{K} \mathbf{q} = \mathbf{Q}, \quad (15)$$

where \mathbf{K} is the stiffness matrix described by equation (13), \mathbf{q} is an unknown vector of displacements and \mathbf{Q} is a vector of nodal forces. In the case of dynamic problem, the eigenproblem is analyzed for an undamped system:

$$(\mathbf{K} - \omega^2 \mathbf{M}) \mathbf{v} = \mathbf{0} \quad (16)$$

and for damped system:

$$(\mathbf{L}_1 - s \mathbf{L}_2) \mathbf{v} = \mathbf{0}, \quad (17)$$

where

$$\mathbf{L}_1 = \begin{bmatrix} -\mathbf{K} & \mathbf{0} \\ \mathbf{0} & \mathbf{M} \end{bmatrix}, \quad \mathbf{L}_2 = \begin{bmatrix} \mathbf{C} & \mathbf{M} \\ \mathbf{M} & \mathbf{0} \end{bmatrix}. \quad (18)$$

\mathbf{K} is the same as in equation (15) and \mathbf{M} is the mass matrix described by equation (14), \mathbf{v} is an eigenvector, and ω is natural frequency. In the case of damped systems, \mathbf{C} is the damping matrix described as $\mathbf{C} = a_1 \mathbf{K} + a_2 \mathbf{M}$, where a_1 and a_2 are the coefficients of Rayleigh damping. The natural frequency and nondimensional damping ratio can be calculated as:

$$\omega = \mu^2 + \eta^2, \quad \gamma = -\mu/\omega, \quad (19)$$

where $\mu = \text{Re}(s)$ and $\eta = \text{Im}(s)$.

3. NUMERICAL EXAMPLES

For numerical analyses, a circular arch with a span $B = 20$ m was selected (Fig. 2). Several arches of different heights H were analyzed, each time adjusting the radius of curvature R so that the arch span B was always the same.

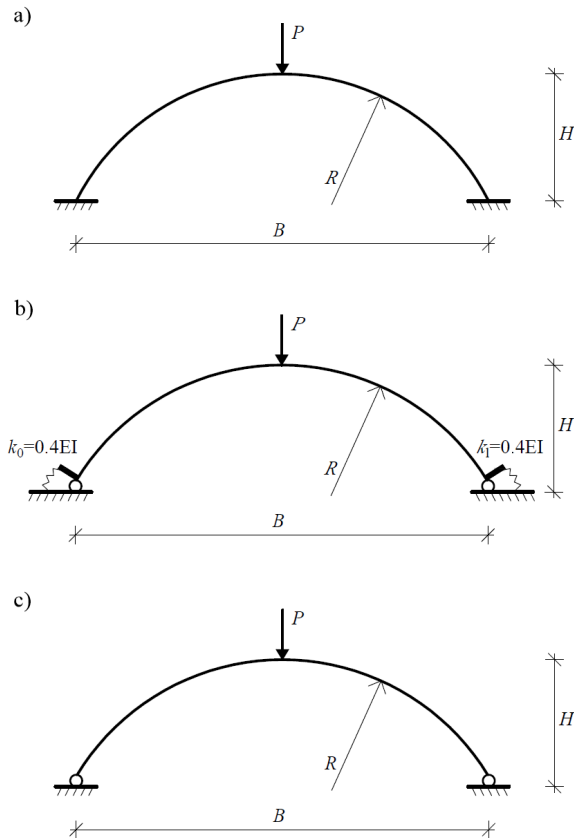


Fig. 2. Circular arch structures with span B supported in various ways: a) clamped-clamped, b) flexible-flexible, c) pinned-pinned

In all analyses, a rectangular cross-section with dimensions $b \times h = 0.4 \times 0.6$ m was used and it was assumed that the structure was made of C25/30 concrete, for which Young's modulus $E = 31.0$ GPa. The considered structures had elastic supports at both ends, for which the values of the rotational stiffness coefficients were changed. The values of the rotational stiffness coefficients were determined in relation to the bending stiffness of the analyzed element EI . Therefore, when the stiffness of the flexible supports tends to infinity, the obtained solution corresponds to the clamped-clamped system, while when the stiffness tends to zero, a solution for the pinned-pinned structure is obtained. The proposed approach was also used to analyze arches with internal connections, in which the variable was elastic rotational stiffness.

3.1. Solution convergence analysis

First, the convergence of the solution obtained with the use of curved elements was carried out and compared with the solution obtained with the use of straight elements.

The solution convergence analysis was carried out for a circular arch with a height of $H = 10$ m and a span of $B = 20$ m, in which various division into finite elements were used. Both supports were assumed to be clamped C-C ($k_0 = k_1 = \infty$), flexible F-F ($k_0 = k_1 = 0.4EI$) or pinned P-P ($k_0 = k_1 = 0$).

The results of dynamic calculations were used for the tests, i.e., the first three natural frequencies for systems supported in different ways (Table 1). The results obtained for the arch di-

Table 1

Natural frequencies ω_i [Hz] of arch structure for different numbers of finite elements

Type of supports	Mode i	$n = 4$	Error [%]	$n = 8$	Error [%]	$n = 64$ Reference
C-C	1	4.2309	0.12	4.2267	0.02	4.2257
	2	9.2793	0.65	9.2336	0.15	9.2198
	3	17.7317	3.99	17.1371	0.50	17.0516
F-F	1	3.3021	0.08	3.3001	0.02	3.2996
	2	7.8253	0.52	7.7929	0.11	7.7845
	3	15.2528	3.16	14.8449	0.40	14.7853
P-P	1	2.1945	0.04	2.1939	0.01	2.1937
	2	6.6992	0.42	6.6767	0.08	6.6713
	3	13.7717	2.68	13.4601	0.35	13.4129

vided into 64 elements were adopted as the most accurate, i.e., the reference solution.

The relative error was calculated as the difference in the solutions related to the reference solution. The use of a curved finite element in the dynamic analysis of arch structures allows for a significant reduction in the number of finite elements without deteriorating the results. Even when the system is divided into 4 elements, the first natural frequencies differ from the reference solution by less than one percent.

A similar analysis of the convergence was performed for the arch discretized with straight finite elements. Also, in this case, the first three natural frequencies were determined for the systems supported in different ways (Table 2).

Table 2

Natural frequencies ω_i [Hz] of arch structure for different numbers of finite elements n – straight finite beam element

Type of supports	Mode i	$n = 4$	Error [%]	$n = 10$	Error [%]	$n = 50$ Reference
C-C	1	4.5294	6.50	4.3023	1.16	4.2529
	2	9.8736	5.91	9.4336	1.19	9.3222
	3	23.1914	33.78	17.5650	1.33	17.3350
F-F	1	3.5954	8.49	3.3592	1.36	3.3141
	2	8.7945	12.09	7.9920	1.87	7.8456
	3	20.918	39.77	15.2590	1.96	14.966
P-P	1	2.5129	14.20	2.2471	2.12	2.2004
	2	7.8109	16.37	6.8694	2.35	6.7119
	3	19.1890	41.60	13.8610	2.28	13.5520

In the case of modeling the arch with straight elements, the convergence of the solution is slower.

3.2. System with a number of flexible joints

The proposed approach makes it possible to solve the static and dynamic problems of arch structures with any number of flexible joints that can be freely distributed along the system (Fig. 3).

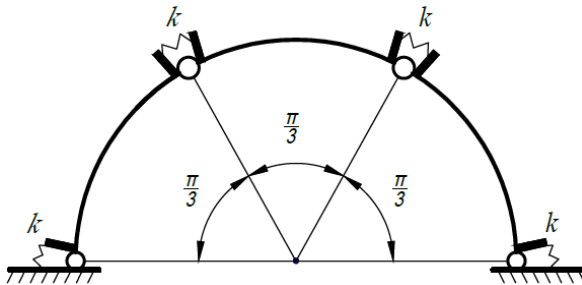


Fig. 3. Circular arch with four flexible joints

Table 3 compares the results of dynamic calculations, i.e., the first three natural frequencies for the systems: without flexible nodes (C–C), with two flexible joints in the supports (F–F) and for the system with four flexible joints shown in Fig. 3. The value of the rotational stiffness coefficient was the same in all flexible joints, i.e., $k = 0.4EI$.

Table 3

Natural frequencies ω_i [Hz] of arch structure with different numbers of flexible joints

Mode i	C–C	F–F	Four nodes
1	4.2267	3.3001	3.0262
2	9.2336	7.7929	7.7830
3	17.1371	14.8449	13.6697

The most visible change in the solution was achieved after introducing a flexible joint to the arch structure (the difference between solution ω_1 for a structure with flexible supports and the solution for an arch with rigid nodes is over 20%) while increasing the number of flexible joints slightly changes the solution.

4. PARAMETRIC STUDY AND DISCUSSION

4.1. Influence of axial and shear forces

The circular arch with a span of $B = 20$ m and a height of $H = 4$ m was loaded in the middle of the span with a concentrated force of $P = 10$ kN (Fig. 2). The Kirchhoff modulus is $G = 11.654$ GPa. Moreover, taking into account the length of finite element l_e (division into 8 elements) and the cross-section factor $\kappa = 5/6$, the coefficient expressing the influence of shear forces $d = 0.0062096$ and the coefficient expressing the influence of axial forces $e = 0.0019454$ were determined. Table 4 shows the results, vertical displacements caused by a point force, obtained for the arch structures depending on the type of support, with ($d \neq 0, e \neq 0$) or without ($d = 0, e = 0$) taking into

account the influence of shear or axial forces. Dimensionless displacement values were given in relation to the arch length, i.e. $\bar{\delta} = \delta/L \cdot 10^5$, where δ is the vertical displacement in the center of the arch and L is the length of the arch.

Table 4

Vertical dimensionless displacements $\bar{\delta}$ in the center of the arch for various supports

Type of supports	$d \neq 0$ $e \neq 0$	$d = 0$ $e \neq 0$	$d \neq 0$ $e = 0$	$d = 0$ $e = 0$	SBE
C–C	0.9660	0.9373	0.7639	0.7344	0.9059
F–F	1.1487	1.1226	0.9805	0.9542	1.0669
P–P	1.2900	1.2648	1.1457	1.1205	1.1926

In addition to the results obtained with the use of curved finite elements, Table 4 also shows the results for an arch modeled with straight beam elements (SBE). For each type of structure support, higher values of displacements were obtained after taking into account the influence of shear or axial forces in the calculations. For the SBE model, the displacements are also smaller than for a curved element in which all influences are included. This suggests the necessity to use an approach that takes into account these influences.

Then, the arches supported in various ways were subjected to dynamic analysis. Table 5 presents the results, the first three natural frequencies obtained with or without taking into account the influence of shear or axial forces.

Table 5

Natural frequencies ω_i of arch structures [Hz]

Type of supports	Mode i	$d \neq 0$, $e \neq 0$	$d = 0$, $e \neq 0$	$d \neq 0$, $e = 0$	$d = 0$, $e = 0$	SBE
C–C	1	11.0519	11.1691	11.0577	11.1795	11.2118
	2	19.9160	20.2265	20.8715	21.2688	20.4545
	3	36.5374	36.5403	37.3457	38.3654	37.9407
F–F	1	8.6859	8.7401	8.6914	8.7481	8.7855
	2	17.1742	17.3446	17.5776	17.7797	17.6028
	3	32.2394	32.7299	32.1069	32.6837	32.9887
P–P	1	6.7922	6.8176	6.7966	6.8235	6.8665
	2	15.6148	15.7341	15.8145	15.9512	15.9766
	3	29.9394	30.3168	29.8120	30.2600	30.5839

Then the damped system is considered and in Table 6 the nondimensional damping ratio for different supports is shown. The Rayleigh coefficients are $a_1 = 0.0001$ and $a_2 = 0.001$.

Tables 5 and 6 show the effect of introducing the flexibility of supports on the results.

Table 6
Nondimensional damping ratio γ_i of arch structures

Type of supports	Mode i	$d \neq 0, e \neq 0$	$d = 0, e \neq 0$	$d \neq 0, e = 0$	$d = 0, e = 0$	SBE
C-C	1	0.0382	0.0386	0.0382	0.0386	0.0387
	2	0.0688	0.0699	0.0721	0.0735	0.0708
	3	0.1263	0.1263	0.1291	0.1326	0.1339
F-F	1	0.0300	0.0302	0.0300	0.0302	0.0303
	2	0.0593	0.0599	0.0607	0.0614	0.0609
	3	0.1114	0.1131	0.1110	0.1129	0.1133
P-P	1	0.0235	0.0236	0.0235	0.0236	0.0237
	2	0.0540	0.0544	0.0547	0.0551	0.0553
	3	0.1035	0.1048	0.1030	0.1046	0.1059

4.2. The influence of rotational elasticity

This analysis covered arches in which only one support node has a given rotational elasticity. The rotational stiffness coefficient $k_0 = \beta_1 \cdot EI$, where EI is the bending stiffness of the bar, and β_1 is the parameter, was gradually increased, starting from zero. Figure 4 shows the selected results, vertical displacements caused by a concentrated force, obtained for arch structures of different heights H but the same span B . The results can be summarized that, regardless of the height of the arch H , for a rotational stiffness twice as high as the bending stiffness of the bar element ($k_0 = 2 \cdot EI$), the solutions correspond to the structure with rigid supports.

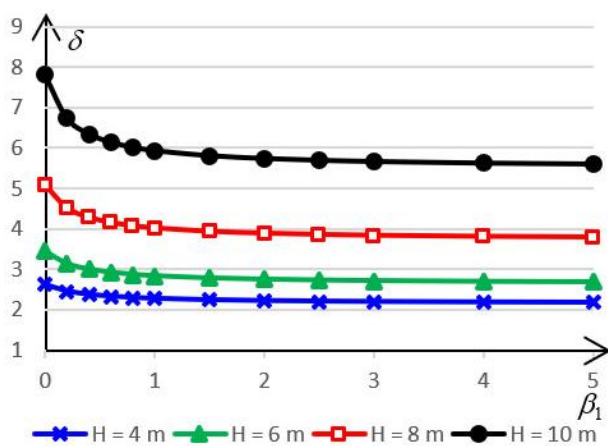


Fig. 4. Vertical displacement $\delta [\times 10^{-4} \text{ m}]$ as a function of the rotational stiffness coefficient $k_0 = \beta_1 \cdot EI$ for arches of different heights

A similar analysis, i.e., the influence of the arch height and the rotational stiffness of the support node on the solution, was performed for the dynamic problem. Figure 5 shows the diagram of changes in the natural frequency ω_1 , for arches of different heights, as functions dependent on the rotational stiffness coefficient of one support $k_0 = \beta_1 \cdot EI$.

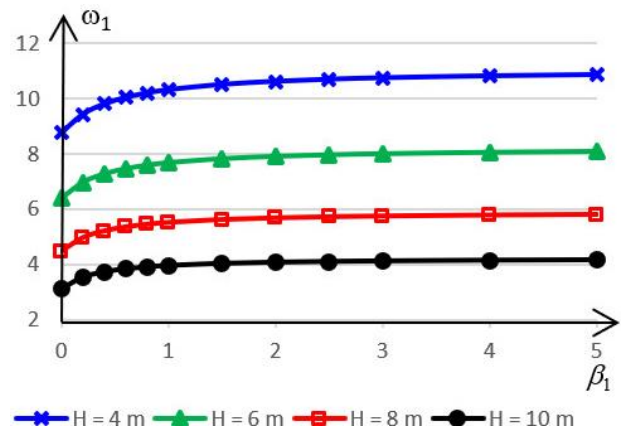


Fig. 5. The first natural frequency ω_1 depending on the coefficient of rotational stiffness of the support $k_0 = \beta_1 \cdot EI$

For all analyzed arch heights H , when the rotational stiffness of the node exceeds twice the bending stiffness of the element ($\beta_1 = 2$), the change in solution is relatively small and the structure can be considered as rigidly supported.

4.3. The position of the flexible joint

In this part, circular arches with constant height $H = 10 \text{ m}$ and span $B = 20 \text{ m}$ were analyzed, in which there was only one flexible joint, but its location in the structure was freely chosen. The position of the joint with a given rotational elasticity was determined by the angle α_1 , which was between the radius passing through the flexible node and the radius passing through the support node (Fig. 6).

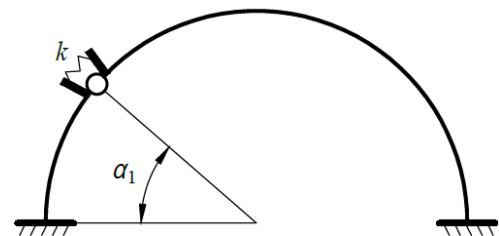


Fig. 6. Circular arch with one flexible joint

The value of the rotational stiffness coefficient k was gradually increased until the change in the solution was relatively small.

Figure 7 shows the results of static calculations, vertical displacements caused by the vertical force, obtained for different positions of the flexible node, i.e., different values of the angle α_1 .

On the basis of the obtained results, it can be concluded that when the flexible node is located at the angle $\alpha_1 = 3\pi/8$, the value of the vertical displacement caused by the force applied in the center of the arch is the same regardless of the value of the rotational stiffness coefficient k . Figure 8 shows the results of dynamic calculations, the values of the first natural frequency ω_1 , obtained for different positions of the flexible node, for the increasing value of the rotational stiffness coefficient k_0 .

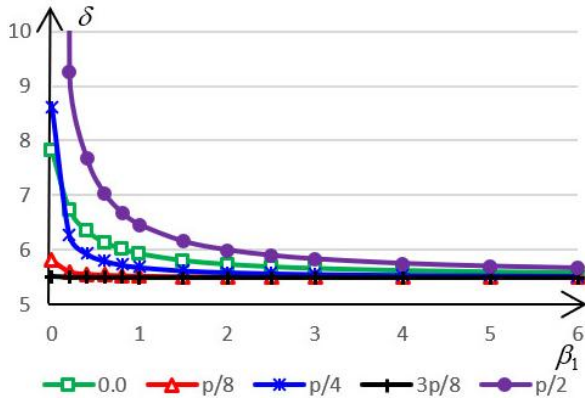


Fig. 7. Vertical displacement $\delta [\times 10^{-4} \text{ m}]$ versus the rotational stiffness coefficient $k = \beta_1 \cdot EI$ for different flexible node positions

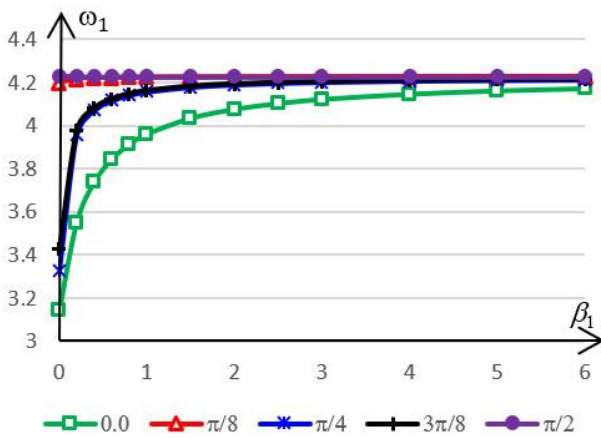


Fig. 8. The first natural frequency ω_1 versus the rotational stiffness coefficient $k = \beta_1 \cdot EI$ for different elastic node positions

The results of dynamic calculations show that the value of the first natural frequency is almost constant for the elastic joint located at the top of the arch, for any value of the rotational stiffness coefficient k .

5. CONCLUSIONS

The paper presents an analysis of arch structures that were modeled with the use of curved finite elements. The proposed method makes it possible to take into account the influence of shear and axial forces, as well as to consider the influence of rotational flexibility of joints on the static and dynamic parameters of the considered structures. The presented approach allows for the analysis of the structure in which there are flexible nodes not only in the supports but also at any point along the considered system and their number can be arbitrary. Based on the analyses performed, the following conclusions can be drawn.

Taking into account the influence of shear or axial force in the static or dynamic analysis of the considered arches leads to a slight increase in the value of the displacements and natural frequencies.

Regardless of the arch height, for the rotational stiffness coefficient of a flexible joint at least twice as much as the bending

stiffness of the structure bar itself, solutions corresponding to structures with rigid supports are obtained.

The conducted analyses have shown that for the considered arches there are certain positions of the elastic joint for which the static or dynamic results are almost constant, regardless of the value of the joint rotational stiffness coefficient.

APPENDIX 1

The stiffness matrix for the circular curved element is as follows:

$$\bar{\mathbf{K}} = \frac{EI}{l^3} [\bar{k}_{ij}]_{6 \times 6}, \quad (\text{A1})$$

where

$$\bar{k}_{11} = \alpha^4 (D' + D''c), \quad \bar{k}_{12} = \alpha^4 D''s,$$

$$\bar{k}_{13} = -\alpha^3 (D' + D''c) + \frac{2\alpha^2 s}{D_1}, \quad \bar{k}_{14} = -\alpha^4 (D'c + D''),$$

$$\bar{k}_{15} = \alpha^4 D's, \quad \bar{k}_{16} = \alpha^3 (D'c + D'') - \frac{2\alpha^2 s}{D_1},$$

$$\bar{k}_{22} = \alpha^4 (D' - D''c), \quad \bar{k}_{23} = -\alpha^3 D''s + \frac{2\alpha^2(1-c)}{D_1},$$

$$\bar{k}_{24} = -k_{15}, \quad \bar{k}_{25} = -\alpha^4 (D'c - D''),$$

$$\bar{k}_{26} = \alpha^3 D's - \frac{2\alpha^2(1-c)}{D_1},$$

$$\bar{k}_{26} = \alpha^2 (D' + D''c) + 1 + \frac{4(1-c-\alpha s)}{D_1},$$

$$\bar{k}_{34} = \bar{k}_{16}, \quad \bar{k}_{35} = -\bar{k}_{26},$$

$$\bar{k}_{36} = -\alpha^2 (D'c + D'') - 1 - \frac{4(1-c-\alpha s)}{D_1},$$

$$\bar{k}_{44} = \bar{k}_{11}, \quad \bar{k}_{45} = -\bar{k}_{12}, \quad \bar{k}_{46} = \bar{k}_{13},$$

$$\bar{k}_{55} = \bar{k}_{22}, \quad \bar{k}_{56} = -\bar{k}_{23}, \quad \bar{k}_{66} = \bar{k}_{33},$$

where

$$s = \sin \alpha, \quad s_0 = \sin \alpha_0, \quad c = \cos \alpha, \quad c_0 = \cos \alpha_0,$$

$$d_1 = \alpha^2 d, \quad e_1 = \alpha^2 e, \quad \alpha = 2\alpha_0,$$

$$D_1 = \alpha(\alpha + \sin \alpha)(1 + d_1 + e_1) - 2[2(1 - \cos \alpha) + \alpha d_1 \sin \alpha],$$

$$D_2 = \alpha(\alpha + \sin \alpha)(1 + d_1 + e_1) - 2\alpha \sin \alpha(1 + e_1),$$

$$D' = \frac{1}{D_1} + \frac{1}{D_2}, \quad D'' = \frac{1}{D_1} - \frac{1}{D_2}.$$

The consistent mass matrix for the circular curved element is the following:

$$\bar{\mathbf{M}} = \rho R [\bar{m}_{ij}]_{6 \times 6}, \quad (\text{A2})$$

where

$$\bar{m}_{ij} = \bar{m}_{ij}^1 + \bar{m}_{ij}^2 + \frac{l^2}{2} \bar{m}_{ij}^3.$$

Components m_{ij}^1 and m_{ij}^2 can be determined by the following formulas:

$$\begin{aligned} \bar{m}_{ij}^k &= 2\alpha_0 C_{0i}^k C_{0j}^k + 2s_0 \left(C_{0i}^k C_{3j}^k + C_{3i}^k C_{0j}^k \right) \\ &+ 2(s_0 - \alpha_0 c_0) \left(C_{0i}^k C_{4j}^k + C_{4i}^k C_{0j}^k + C_{1i}^k C_{2j}^k + C_{2i}^k C_{1j}^k \right) \\ &+ \frac{2}{3} \alpha_0^3 C_{1i}^k C_{1j}^k + (\alpha_0 - s_0 c_0) C_{2i}^k C_{2j}^k + (\alpha_0 + s_0 c_0) C_{3i}^k C_{3j}^k \\ &+ 2(\alpha_0^2 s_0 + 2\alpha_0 c_0 - 2s_0) \left(C_{1i}^k C_{5j}^k + C_{5i}^k C_{1j}^k \right) \\ &+ \left[\alpha_0 \left(\frac{1}{2} - c_0^2 \right) + \frac{1}{2} s_0 c_0 \right] \\ &\cdot \left(C_{2i}^k C_{5j}^k + C_{5i}^k C_{2j}^k + C_{3i}^k C_{4j}^k + C_{4i}^k C_{3j}^k \right) \\ &+ \left[\frac{1}{2} \alpha_0^3 - \alpha_0^2 s_0 c_0 + \alpha_0 \left(\frac{1}{2} - c_0^2 \right) + \frac{1}{2} s_0 c_0 \right] C_{4i}^k C_{4j}^k \\ &+ \left[\frac{1}{3} \alpha_0^3 + \alpha_0^2 s_0 c_0 - \alpha_0 \left(\frac{1}{2} - c_0^2 \right) - \frac{1}{2} s_0 c_0 \right] C_{5i}^k C_{5j}^k, \end{aligned}$$

where:

$$\begin{aligned} C_{01}^1 &= C_{04}^1 = -\frac{\alpha s}{D_2}, \quad C_{11}^1 = -C_{14}^1 = -\frac{2s}{D_1}, \\ C_{21}^1 &= -C_{24}^1 = -\frac{A_2 \alpha c_0}{2} (D'c + D'') \\ &+ \frac{2c_0}{D_1} (\alpha + s) - \frac{A_1 \alpha^2 s_0}{2D_2}, \\ C_{31}^1 &= C_{34}^1 = \frac{A_2 \alpha s_0}{2} (D'c + D'') \\ &+ \frac{2\alpha s_0}{D_2} + \frac{A_1 \alpha^2 c_0}{2D_1} - \frac{2s_0 s}{D_1}, \\ C_{41}^1 &= C_{44}^1 = \frac{A_1 \alpha s_0}{D_2}, \quad C_{51}^1 = -C_{54}^1 = -\frac{A_1 \alpha c_0}{D_1}, \\ C_{01}^2 &= -C_{04}^2 = -\frac{2s}{D_1}, \quad C_{11}^2 = C_{14}^2 = 0, \\ C_{21}^2 &= C_{24}^2 = -\frac{A_1 \alpha^2 c_0}{2D_1} - \frac{D' A_2 c_0 \alpha s}{2} + \frac{2s_0 s}{D_1}, \\ C_{31}^2 &= -C_{34}^2 = -\frac{A_1 \alpha^2 s_0}{2D_2} - \frac{D' A_2 s_0 \alpha s}{2} + \frac{2c_0 s}{D_1}, \\ C_{41}^2 &= -C_{44}^2 = \frac{A_1 \alpha c_0}{D_1}, \quad C_{51}^2 = C_{54}^2 = \frac{A_1 \alpha s_0}{D_2}, \\ C_{01}^3 &= C_{04}^3 = -\frac{\alpha^2 s}{D_2}, \quad C_{11}^3 = -C_{14}^3 = -\frac{2\alpha s}{D_1}, \\ C_{21}^3 &= -C_{24}^3 = \frac{2\alpha^2 c_0}{D_1}, \quad C_{31}^3 = C_{34}^3 = \frac{2\alpha^2 s_0}{D_2}, \\ C_{41}^3 &= C_{44}^3 = 0, \quad C_{51}^3 = -C_{54}^3 = 0, \\ C_{02}^1 &= -C_{05}^1 = \frac{\alpha(1+c)}{D_2}, \quad C_{12}^1 = C_{15}^1 = -\frac{2(1-c)}{D_1}, \\ C_{22}^1 &= C_{25}^1 = -\frac{D' A_2 c_0 \alpha s}{2} + \frac{2}{D_1} [\alpha s_0 + (1-c)c_0] + \frac{A_1 \alpha^2 c_0}{2D_2}, \\ C_{32}^1 &= -C_{35}^1 = \frac{D' A_2 s_0 \alpha s}{2} - 2 \left[\frac{(1-c)s_0}{D_1} + \frac{\alpha c_0}{D_2} \right] + \frac{A_1 \alpha^2 s_0}{2D_1}, \end{aligned}$$

$$\begin{aligned} C_{42}^1 &= -C_{45}^1 = -\frac{A_1 \alpha c_0}{D_2}, \quad C_{52}^1 = C_{55}^1 = -\frac{A_1 \alpha s_0}{D_1}, \\ C_{02}^2 &= C_{05}^2 = -\frac{2(1-c)}{D_1}, \quad C_{12}^2 = -C_{15}^2 = 0, \\ C_{22}^2 &= -C_{25}^2 = \frac{A_2 \alpha c_0}{2} (D'c - D'') - \frac{A_1 \alpha^2 s_0}{2D_1} + \frac{2(1-c)s_0}{D_1}, \\ C_{32}^2 &= C_{35}^2 = \frac{A_1 \alpha^2 c_0}{2D_2} - \frac{A_2 \alpha s_0}{2} (D'c - D'') + \frac{2(1-c)c_0}{D_1}, \\ C_{42}^2 &= C_{45}^2 = \frac{A_1 \alpha s_0}{D_1}, \quad C_{52}^2 = -C_{55}^2 = -\frac{A_1 \alpha c_0}{D_2}, \\ C_{02}^3 &= -C_{05}^3 = \frac{\alpha^2(1+c)}{D_2}, \quad C_{12}^3 = C_{15}^3 = -\frac{2\alpha(1-c)}{D_1}, \\ C_{22}^3 &= C_{25}^3 = \frac{2\alpha^2 s_0}{D_1}, \quad C_{32}^3 = -C_{35}^3 = -\frac{2\alpha^2 c_0}{D_2}, \\ C_{42}^3 &= -C_{45}^3 = 0, \quad C_{52}^3 = C_{55}^3 = 0, \\ C_{03}^1 &= C_{06}^1 = \frac{s}{D_2} + \frac{1}{2\alpha}, \\ C_{13}^1 &= -C_{16}^1 = \frac{2}{\alpha^2} \left[\frac{\alpha s}{D_1} - \frac{1}{2} - \frac{2(1-c)}{D_1} \right], \\ C_{23}^1 &= -C_{26}^1 = \frac{A_2 c_0}{2} \left(D'c + D'' - \frac{2s}{\alpha D_1} \right) \\ &+ \frac{2}{D_1} \left(\frac{2}{\alpha} s_0 - c_0 \right) + \frac{A_1 \alpha s_0}{2D_2} + \frac{c_0}{\alpha^2} \left(\frac{4-4c-2\alpha s}{D_1} + 1 \right), \\ C_{33}^1 &= C_{36}^1 = -\frac{A_2 s_0}{2} \left(D'c + D'' - \frac{2s}{\alpha D_1} \right) \\ &- \frac{A_1}{2D_1} (\alpha c_0 - 2s_0) - \frac{2s_0}{D_2} - \frac{s_0}{\alpha^2} \left(\frac{4-4c-2\alpha s}{D_1} + 1 \right), \\ C_{43}^1 &= C_{46}^1 = -\frac{A_1 s_0}{D_2}, \quad C_{53}^1 = -C_{56}^1 = \frac{A_1 (\alpha c_0 - 2s_0)}{\alpha D_1}, \\ C_{03}^2 &= -C_{06}^2 = -\frac{1}{\alpha^2} \left(\frac{4-4c-2\alpha s}{D_1} + 1 \right), \\ C_{13}^2 &= C_{16}^2 = 0, \\ C_{23}^2 &= C_{26}^2 = \frac{A_2 c_0}{2} \left(D's - \frac{2(1-c)}{\alpha D_1} \right) \\ &+ \frac{A_1}{D_1} \left(\frac{\alpha c_0}{2} - s_0 \right) + \frac{s_0}{\alpha^2} \left(\frac{4-4c-2\alpha s}{D_1} + 1 \right), \\ C_{33}^2 &= -C_{36}^2 = -\frac{A_2 s_0}{2} \left(D's - \frac{2(1-c)}{\alpha D_1} \right) \\ &+ \frac{A_1 \alpha s_0}{2D_2} + \frac{c_0}{\alpha^2} \left(\frac{4-4c-2\alpha s}{D_1} + 1 \right), \\ C_{43}^2 &= -C_{46}^2 = -\frac{A_1 (\alpha c_0 - 2s_0)}{\alpha D_1}, \\ C_{53}^2 &= C_{56}^2 = -\frac{A_1 s_0}{D_2}, \quad C_{03}^3 = C_{06}^3 = \frac{\alpha s}{D_2} + \frac{1}{2}, \\ C_{13}^3 &= -C_{16}^3 = -\frac{1}{\alpha} \left(\frac{4-4c-2\alpha s}{D_1} + 1 \right), \\ C_{23}^3 &= -C_{26}^3 = \frac{2(2s_0 - \alpha c_0)}{D_1}, \quad C_{33}^3 = C_{36}^3 = -\frac{2\alpha s_0}{D_2}, \\ C_{43}^3 &= C_{46}^3 = 0, \quad C_{53}^3 = -C_{56}^3 = 0. \end{aligned}$$

ACKNOWLEDGEMENTS

The study has been supported by the University's internal grant No. 0411/SBAD/0006. This support is gratefully acknowledged.

REFERENCES

- [1] J. Henrych, *The dynamics of arches and frames*. Elsevier, 1981.
- [2] I.A. Karnovsky, *The theory of arched structures*. New York, Springer, 2012, doi: [10.1007/978-1-4614-0469-9](https://doi.org/10.1007/978-1-4614-0469-9).
- [3] Z. Friedman and J. Kosmatka, "An accurate two-node finite element for shear deformable curved beams," *Int. J. Numer. Methods Eng.*, vol. 41, pp. 473–498, 1998, doi: [10.1002/\(SICI\)1097-0207\(19980215\)41:3<473::AID-NME294>3.0.CO;2-Q](https://doi.org/10.1002/(SICI)1097-0207(19980215)41:3<473::AID-NME294>3.0.CO;2-Q).
- [4] F. Yang, R. Sedaghatia, and E. Esmailzadeh, "Free in-plane vibration of general curved beams using finite element method," *J. Sound Vibr.*, vol. 318, pp. 850–867, 2008, doi: [10.1016/j.jsv.2008.04.041](https://doi.org/10.1016/j.jsv.2008.04.041).
- [5] H. Stolarski and T. Belytschko, "Shear and membrane locking in curved C^0 elements," *Comput. Meth. Appl. Mech. Eng.*, vol. 41, pp. 279–296, 1983, doi: [10.1016/0045-7825\(83\)90010-5](https://doi.org/10.1016/0045-7825(83)90010-5).
- [6] P. Raveendranath, S. Gajbir, and B. Pradhan, "Free vibration of arches using a curved beam element based on a coupled polynomial displacement," *Comput. Struct.*, vol. 78, pp. 583–590, 2000, doi: [10.1016/S0045-7949\(00\)00038-9](https://doi.org/10.1016/S0045-7949(00)00038-9).
- [7] P. Litewka and J. Rakowski, "The exact thick arch finite element," *Comput. Struct.*, vol. 68, pp. 369–379, 1998, doi: [10.1016/S0045-7949\(98\)00051-0](https://doi.org/10.1016/S0045-7949(98)00051-0).
- [8] X. Tong, N. Mrad, and B. Tabarrok, "In-plane vibration of circular arches with variable cross-section," *J. Sound Vibr.*, vol. 212, no. 1, pp. 121–140, 1998, doi: [10.1006/jsvi.1997.1441](https://doi.org/10.1006/jsvi.1997.1441).
- [9] H. Öztürk, I. Yesilyurt, and M. Sabuncu, "In-plane stability analysis of non-uniform cross-sectioned curved beams," *J. Sound Vibr.*, vol. 296, pp. 277–291, 2006, doi: [10.1016/j.jsv.2006.03.002](https://doi.org/10.1016/j.jsv.2006.03.002).
- [10] A. Borković, B. Marussig, and G. Radenković, "Geometrically exact static isogeometric analysis of an arbitrarily curved spatial Bernoulli-Euler beam," *Comput. Meth. Appl. Mech. Eng.*, vol. 390, p. 114447, 2022, doi: [10.1016/j.cma.2021.114447](https://doi.org/10.1016/j.cma.2021.114447).
- [11] A.T. Luu, N.I. Kim, and J. Lee, "Isogeometric vibration analysis of free-form Timoshenko curved beams," *Meccanica*, vol. 50, pp. 169–187, 2015, doi: [10.1007/s11012-014-0062-3](https://doi.org/10.1007/s11012-014-0062-3).
- [12] S.M. Lin and S.Y. Lee, "Closed-form solutions for dynamic analysis of extensional circular Timoshenko beams with general elastic boundary conditions," *Int. J. Solids Struct.*, vol. 38, pp. 227–240, 2001, doi: [10.1016/S0020-7683\(00\)00020-2](https://doi.org/10.1016/S0020-7683(00)00020-2).
- [13] Y.B. Yang, C.L. Lin, J.D. Yau, and D.W. Chang, "Mechanism of resonance and cancellation for train-induced vibrations on bridges with elastic bearings," *J. Sound Vibr.*, vol. 269, pp. 345–360, 2004, doi: [10.1016/S0022-460X\(03\)00123-8](https://doi.org/10.1016/S0022-460X(03)00123-8).
- [14] C. Zhuo, S.X. Xiang, and Y. Yingjie, "Modal research of underground arch structure with elastic support," *J. Phys. Conf. Ser.*, vol. 1972, p. 012131, 2021, doi: [10.1088/1742-6596/1972/1/012131](https://doi.org/10.1088/1742-6596/1972/1/012131).
- [15] M. Sekulovic, R. Salatic, and M. Nefrovska, "Dynamic analysis of steel frames with flexible connections," *Comput. Struct.*, vol. 80, pp. 935–955, 2002, doi: [10.1016/S0045-7949\(02\)00058-5](https://doi.org/10.1016/S0045-7949(02)00058-5).
- [16] A.U. Öztürk, H.M. Catal, "Dynamic analysis of semi-rigid frames," *Math. Comput. Appl.*, vol. 10, no. 1, pp.1–8, 2005, doi: [10.3390/mca10010001](https://doi.org/10.3390/mca10010001).
- [17] J. Rakowski, *Exact curved elements in the finite element and boundary element methods*, Poznań, Wydawnictwo Politechniki Poznańskiej, 2011. (in Polish)